

August 2008

Atomistic tight binding study of strain-reduced confinement potentials in identical and non-identical InAs/GaAs vertically stacked quantum dots

Muhammad Usman
Purdue University - Main Campus

Shaikh Ahmed
Southern Illinois University

Gerhard Klimeck
Purdue University - Main Campus, gekco@purdue.edu

Follow this and additional works at: <https://docs.lib.purdue.edu/nanodocs>

Usman, Muhammad; Ahmed, Shaikh; and Klimeck, Gerhard, "Atomistic tight binding study of strain-reduced confinement potentials in identical and non-identical InAs/GaAs vertically stacked quantum dots" (2008). *Other Nanotechnology Publications*. Paper 143.
<https://docs.lib.purdue.edu/nanodocs/143>

This document has been made available through Purdue e-Pubs, a service of the Purdue University Libraries. Please contact epubs@purdue.edu for additional information.

Atomistic tight binding study of strain-reduced confinement potentials in identical and non-identical InAs/GaAs vertically stacked quantum dots

Muhammad Usman¹, Shaikh Ahmed² and Gerhard Klimeck^{1,3}

Abstract - Strain and electronic structure of InAs/GaAs quantum dot molecules made up of identical and non-identical vertically stacked quantum dots are compared using the $sp^3d^5s^*$ nearest neighbor empirical tight binding model. Hydrostatic and biaxial strain profiles strongly impact the local band edges and electronic structure for both identical and non-identical dots. Strain in the lower dot is significantly different as compared to the upper dot in the non-identical system in contrast to the identical system where it is almost the same in both dots. Therefore structural detailed differences are of critical importance and cannot be neglected. Qualitatively, the electronic structure is similar in identical and non-identical dot systems for small separations (below 6nm) and it is significantly different for large separations. The molecular orbitals convert to the dot-localized atomic orbitals at large dot separations in the non-identical system. Non-idealities such as strain and size variations induce an energy splitting in the considered dot ground states. Larger dissimilarity of dots increases $e1-e2$ and decreases the optical gap of system. This favors the possible use of such system in the construction of the long wavelength optical laser.

I - INTRODUCTION AND METHOD

For quite some time, InAs/GaAs quantum dot (QD) and coupled quantum dot systems have attracted attention for various optical [1] and quantum computing applications [2]. Due to the strain, originating from the assembly of lattice-mismatched semiconductors the quantum dot arrays tend to stack in the vertical direction [3, 4] with upper dots slightly larger in size [4]. Such systems are inhomogeneous in material composition and strain. The simulation domain needs to contain 5–50 million atoms in total, where crystal symmetry and atomistic details of interfaces are extremely important [5, 6]. Most of the work previously done [5, 7] to analyze such closely coupled systems used continuum models such as effective mass and $k \cdot p$ which ignore such crystal symmetry and atomistic resolution. Only recently, an atomistic approach and pseudo-potential method for identical [8, 9, 11] and non-identical dots have been used [10, 11].

In this paper, a detailed description of strain and electronic structure of closely coupled identical and non-identical quantum dot systems is presented using NEMO 3-D [12]. NEMO 3-D can atomistically simulate realistic systems as large as containing up to 52 million atoms [13, 14]. The electronic structure is calculated using a twenty band $sp^3d^5s^*$ nearest neighbor empirical tight binding model [15] and the strain with an atomistic valence force field (VFF) method [16].

In the past, the NEMO 3-D basis set and approach have been validated through experimentally verified: 1) high bias, high current, quantitative resonant tunneling diode modeling [17], 2) photoluminescence in InAs nanoparticles [18], 3) modeling of the Stark effect of single P impurities in Si [19], 4) the valley splitting in miscut Si quantum wells on SiGe substrate [20], and 5) the strain and piezoelectric effects on the electronic structure of single InAs/GaAs quantum dots [22]. Here NEMO 3-D is used for the study of the stacked QD physics in realistically sized systems.

Hydrostatic and biaxial strain impacts on electronic structure of non-identical and identical quantum dots are compared which have not been done previously. Experimentally it is very hard to control the size of the quantum dots during the fabrication. It has been shown experimentally that the quantum dots increase in the size when grow in the vertical direction [4]. Also sometimes, the quantum dots are intentionally grown in different sizes so that to analyze them separately [26] for different strain couplings. To provide a quantitative analysis, the electronic structure of the quantum dot stacks made up of identical and non-identical quantum dots is compared. The electronic structures for the two stacked QDs which are identical and non-identical are similar at small separations ($\sim 6\text{nm}$) and become significantly different at larger than $\sim 8\text{nm}$ separations. This difference of the electronic structure at the large separations may have significant impact on the designing of the quantum gates using coupled quantum dot systems. The difference of the electronic structure is due to the atomistic crystal distortion that is not included in continuum methods and has recently been reported using an atomistic pseudo-potential method [10]. Our results qualitatively confirm the previously published results using an atomistic pseudo potential method, while our approach can scale to significantly larger systems of 52 million atoms [11, 12, 13].

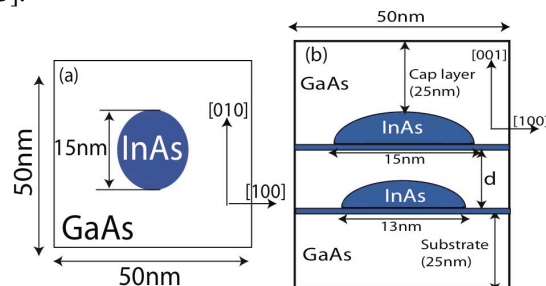


FIG 1: (a) top view and (b) side view of the system simulated. The system is made up of two dome shaped non-identical InAs quantum dots embedded in GaAs buffer. The height of each quantum dot is 3nm. The diameter of upper dot is 15nm and lower dot is 13nm. The quantum dots are surrounded by 50x50 (nm²) GaAs buffer in lateral dimensions. The separation between wetting layers “d” is varied from 4nm to 12nm.

¹School of Electrical and Computer Engineering and Network for Computational Nanotechnology, Purdue University, West Lafayette, IN 47907, USA

²Electrical and Computer Engineering Department, Southern Illinois University, Carbondale, IL 62901, USA

³Jet Propulsion Laboratory, California Institute of Technology, Pasadena, CA 91109

II - SYSTEM SIMULATED

Figure 1 shows the simulated model which consists of two InAs lens shaped quantum dots each with 3nm height on a 1ML InAs wetting layer. The upper dot has a 15nm diameter and the lower dot has a 13nm diameter. A large GaAs buffer (50nm in lateral dimensions and 60nm in [001] direction) around the dots is used to ensure that the strain field vanishes at the buffer boundaries. The electronic structure is computed over a small region extending 20nm above and 15nm lateral to the quantum dots as electron and hole states are confined within the dot regions. The separation between the wetting layers “ d ” has been varied from 4nm to 12nm. This system of different dots is labeled “ D ”. In the case of identical dots, both dots have diameter of 15nm whereas everything else is kept unchanged. This system of equal dots is labeled “ E ”. The largest system simulated ($d=12$ nm) contains 7.9 million atoms and the smallest system ($d=4$ nm) contains 6.8 million atoms in the strain domain. The electronic structure is computed over 3.99 million atoms and 3.37 million atoms for $d=12$ nm and $d=4$ nm respectively.

III - HYDROSTATIC AND BIAxIAL STRAIN

Figure 2 (upper row) shows the trace of the hydrostatic strain $\{e_{xx} + e_{yy} + e_{zz}\}$ for “ D ” through the center of QDs in the [001] direction for several separations “ d ”. For all the cases shown, most of the hydrostatic strain lies within InAs QDs and it is approximately zero outside the dot regions. Even for the 4nm case, the hydrostatic strain magnitude in the GaAs spacer is only $0.0096 \sim 0$. This trend is similar to the identical dot case as shown in Figure 2 (lower row). However, a large top dot increases the strain of the lower dots in non-identical QDs. The lower dot is found to be $\sim 5.8\%$ more hydrostatically strained as compared to the upper dot in non-identical QDs whereas this difference is less than 1% in case of the identical QDs. Hydrostatic strain has direct impact on the electron energy levels and band edges, so these different strain couplings will result in different band edges and electron energy levels.

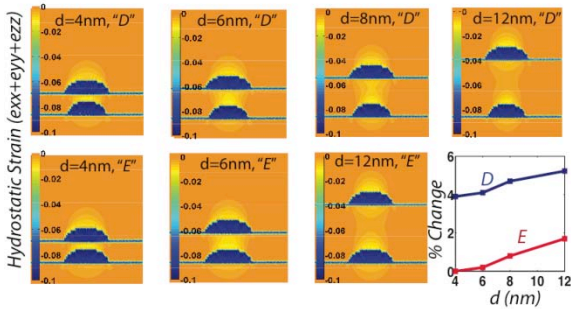


FIG 2: Hydrostatic strain $\{e_{xx} + e_{yy} + e_{zz}\}$ surface plot through the center of QDs in x - z plane. Upper row is for system “ D ” and lower row is for system “ E ” for various GaAs spacer thicknesses “ d ”. The strain is concentrated within QDs and approximately zero outside them. Bottom right most shows the % change in peak value of hydrostatic strain within the lower QD as a function of “ d ”. 4nm spacer is taken as reference.

Figure 3 (a) compares the lowest conduction band edges in “ D ” with increasing separations. Hydrostatic Strain directly shifts the strain modified conduction band edges and reduces the well depth. It is found that well depth reduction for 4nm from the unstrained to strained system is about 510meV, which should be 545meV from a simple analytical model $\{\delta E = -a_c \cdot (e_{xx} + e_{yy} + e_{zz})\}$ using $a_c = -5.08$ for InAs [24]. This has been previously reported as 600meV using effective mass approximation [23]. Further, strain coupling of QDs reduces well depth by 8meV from 12nm to 4nm separation. These long range strain effects are difficult to capture in reduced models like effective mass or $k \cdot p$ [25]. Hence we conclude that atomistic simulation is crucial for understanding of right physics in these complicated multimillion systems.

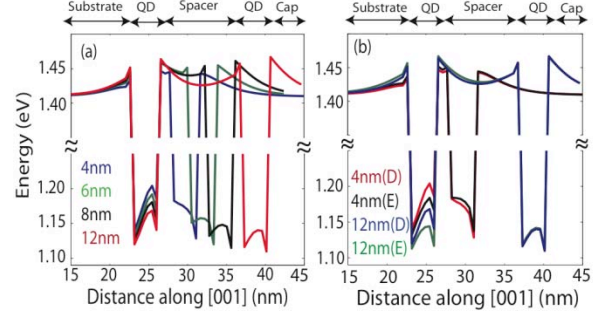


FIG 3: (a) Conduction band edges as a function of distance along [001] direction through the center of QDs in “ D ” for various GaAs spacer thicknesses “ d ”. The band edge moves upward as we reduce the spacer thickness. This is direct consequence of strain coupling. A total 8meV change is calculated for a reduction of “ d ” from 12nm to 4nm. (b) Comparison of conduction band edges plotted as a function of distance along [001] direction through center of QDs in “ D ” and “ E ”. Two extreme values of “ d ” (4nm and 12nm) are taken. Band edges are same in upper dot and are significantly different in lower dot due to different strain effects.

Figure 3 (b) compares the lowest conduction band wells for “ D ” and “ E ”. The results show that well depths for the upper dot are approximately the same because of the same hydrostatic strain whereas the larger hydrostatic strain (about 5.3% more) for the lower dot in “ D ” results in shallower wells (~ 22 meV shallower) thus increasing the confinement. Hence, non-identical dots will have more confined electron states as compared to identical case.

The previous simulations of the quantum dot stacks containing three [12, 21] and seven [11] quantum dots have shown that the strain strongly pushes the ground state to the lower dot in identical quantum dots. In the two dots stack system studied here, this effect is not as pronounced.

Figure 4 plots a biaxial component of the strain given by $\{e_{zz} - (e_{xx} + e_{yy})/2\}$. For all separations in “ D ” and “ E ”, the GaAs spacer is strongly strained and strain penetrates deep into surrounding GaAs buffer. The general trend of biaxial strain is similar for identical and non identical dots. However, strain in the lower dot is $\sim 6.5\%$ lesser than for identical dots which will result in a weak localization of ground hole state in the lower dot as reported in Ref. [23].

The biaxial strain has strong effects on the hole band edges and energy levels. Large positive strain within dots and large negative strain in GaAs spacer will result in strong mixing of heavy hole and light hole band edges as shown in figure 5. The effect is strong enough to create a light hole well

in the GaAs spacer, which is deeper than the light hole well inside the dots. These effects have also been observed for identical dots in Ref. [8, 23]. However, we find that the deep light hole well vanishes more quickly in the non-identical dots as compared to identical dot case. Figure 5 shows that there is almost no light hole well in the InAs QD for GaAs spacer thickness below 8nm. At the 4nm separation, the hole states are a mixture of the heavy hole and the light hole states. For large separations, as the light hole well vanishes in the GaAs spacer between the dots, the ground hole state is totally localized in the upper dot and it has a heavy hole like character.

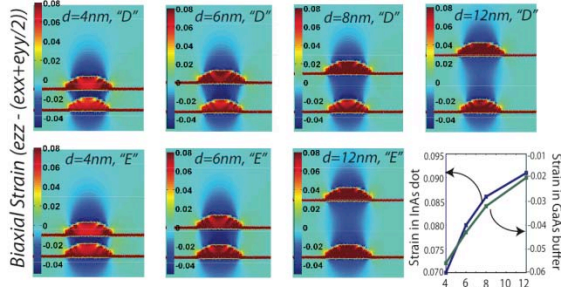


FIG 4: Hydrostatic strain $\{\epsilon_{zz} - (\epsilon_{xx} + \epsilon_{yy})/2\}$ surface plot through the center of QDs in $x-z$ plane. Upper row is for system "D" and lower row is for system "E" for various GaAs spacer thicknesses "d". The strain is concentrated within QDs and approximately zero outside them. Bottom right most shows the % change in peak value of hydrostatic strain within the lower QD as a function of "d". 4nm spacer is taken as reference.

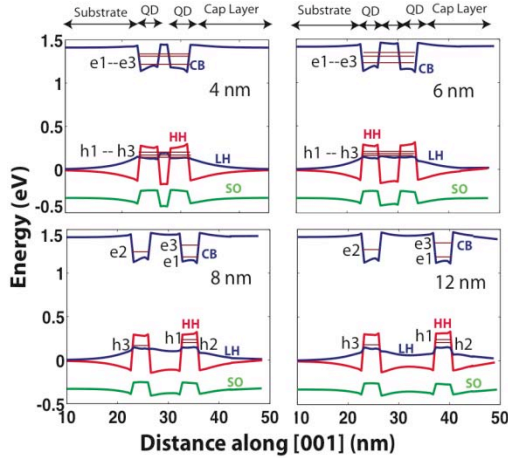


FIG 5: Strain modified band edges along [001] direction as a function of distance through the center of QDs in "D". Only lowest conduction band edge (CB) and heavy hole (HH), light hole (LH) and split off (SO) bands are shown. The horizontal lines marked inside wells show the position of electron and hole energy states of the system. For small separations (4 and 6nm), electron and hole states are molecule like and spread through upper and lower dots. Hole states are a mixture of HH and LH. For separations 8nm and above, electron and hole states show atomic like behavior. The ground electron and hole states are concentrated in upper dot.

IV - ELECTRONIC STRUCTURE

Figure 6(a) compares the six lowest electron energy levels for identical and non-identical dots. The deeper conduction band wells from figure 3(b) for identical dots results in lower values of electron energy levels. For 4nm separation, the difference is ~ 5 meV. It is observed that for small separations (below ~ 6 nm), the electronic structure for

identical and non-identical dots is similar. Strong electronic and strain coupling result in molecular like states. However, as the separation increases above 6nm, the coupling between the QDs becomes weak. As a result, the molecular like states convert to atomic like states for individual dots. The anti-bonding and bonding levels become almost degenerate for "E" ($e1-e2 = 0.8$ meV for $d=12$ nm) whereas the dissimilarity of dots in "D" results in finite difference between the energy levels which further tends to be constant with increasing GaAs spacer thickness. For example in "D", $e1-e2$ is about 16meV for 12nm GaAs spacer. This is almost equal to the difference between states of isolated upper and lower dots which is found to be 16.2meV. Hence, $e1$ and $e2$ becomes s -states of individual dots with $e1$ the s -state of upper dot and $e2$ the s -state of lower dot. Also, the energy levels for single quantum dots were found to be about 22meV below the coupled dot energy levels at 10nm separation. Since, at 10nm distance the electronic coupling is quite small, this difference is attributed to the long-range biaxial strain effect, which penetrates deep into the GaAs buffer. This effect is missing in the effective mass approximation [25], which ignored long-range strain couplings.

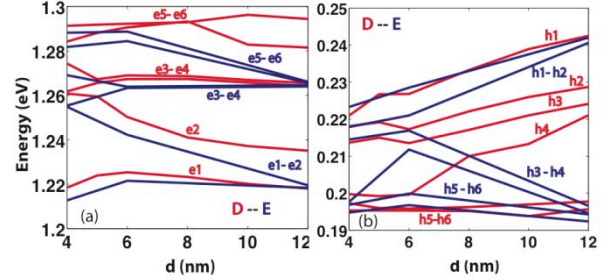


FIG 6: (a) Lowest six electron (b) highest six hole energy states of the system as a function of GaAs spacer thickness "d" in "D" and "E". For small separations below 8nm, the electron state show molecule like behavior. Qualitatively "D" and "E" show same behavior. As the separation increases from 8nm bonding and anti-bonding levels in "E" become almost degenerate (separation ~ 0.8 meV). Dissimilarity of dots in "D" results in finite separation (16.2meV) of $e1$ and $e2$, with $e1$ ground state of upper dot and $e2$ ground state of lower dot. Ground hole state $h1$ increases as "d" is increased reducing the optical gap due to strain coupling of QDs.

Figure 6(b) compares the highest six hole energy levels for identical and non-identical dots. As the separation between the quantum dots is reduced, the ground hole state is pushed to the lower energies i.e. its separation from InAs valence band edge increases. This effect is the direct consequence of the strain as in the absence of the strain the hole ground state is pushed towards the higher energies with decreasing "d" [8]. A reduction of 21.5 meV in "D" and a reduction of 18.7 meV in "E" is calculated when "d" is reduced from 12nm to 4nm.

During the fabrication of QDs, it is very hard to control the exact size of the QDs. Experimentally [4] it has been shown that the QD diameter increases as they grow in vertical direction. The exact difference of the upper and lower dot diameters is unpredictable. E.A. Stinaff et al. [26] fabricated non-identical QDs and analyzed the coupling between them under applied electric field to demonstrate the use of such system for optical information processing. Next we will consider three different configurations of non-identical coupled QDs to quantitatively analyze the size dissimilarity

effect on the electronic structure of such closely coupled systems.

Systems D_{14} , D_{15} , and D_{16} have lower dots with diameter 13nm and upper dot diameter is 14nm, 15nm and 16nm respectively. Figure 7 (a) and (b) plot the first four electron and first three hole energy states as a function of GaAs spacer thickness " d ". Qualitatively, D_{14} , D_{15} and D_{16} show similar trends in the electron and hole energy changes as " d " is changed from 4nm to 12nm. As upper dot diameter increases from 14nm to 16nm, the optical gap reduces and $e1$ - $e2$ separation of the system increases. For example, at " d "=12nm, an optical gap reduction of ~ 26.5 meV and ~ 16.6 meV increase in $e1$ - $e2$ is calculated for " d " varying from 14nm to 16nm. Since $e1$ - $e2$ should be as large as possible for laser applications [27], hence our atomistic tight binding model predicts that D_{16} will be the most suitable topology for the construction of high wavelength optical laser.

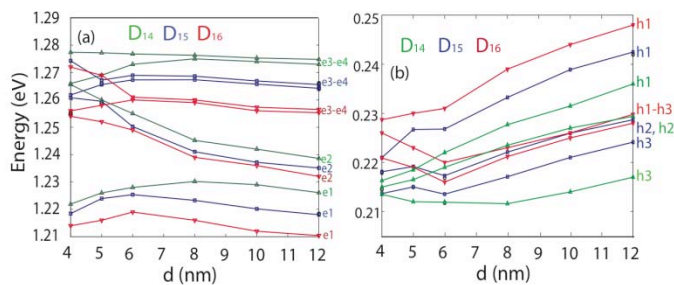


FIG 7: (a) Lowest four electron states are shown as a function of spacer thickness " d ". Three different systems are considered. In all the systems, lower QD has the diameter of 13nm. Upper dot has the diameter of 14nm, 15nm and 16nm in the systems D_{14} , D_{15} and D_{16} respectively. In all the systems, a crossing of $e2$ and $e3$ occurs at 4nm. $e1$ - $e2$ is 8.5meV, 16.2meV and 25.1meV in D_{14} , D_{15} and D_{16} respectively at " d " = 12nm. $e3$ - $e4$ is ~ 0.7 meV in all the systems. (b) Highest three hole states are shown as a function of spacer thickness " d ". Three different systems are considered. In all the systems, lower QD has the diameter of 13nm. Upper dot has the diameter of 14nm, 15nm and 16nm in the systems D_{14} , D_{15} and D_{16} respectively. In all the systems, ground hole energy decreases as the separation of dots is decreased. A reduction of 19.3 meV in D_{14} , 21.5meV in D_{15} and 19.7meV in D_{16} is calculated.

CONCLUSIONS

This work provides a detailed analysis of hydrostatic and biaxial strain in identical and non-identical coupled quantum dot systems. Larger hydrostatic strain ($\sim 5.8\%$ more) causes increased confinement and shallower electron band edges in non-identical dots. Biaxial strain, however, has the opposite trend. Smaller biaxial strain ($\sim 6.5\%$ less) results in lesser mixing of hole band edges as compared to identical dots. Finally it is reported that the electronic structure of identical and non-identical dots is similar at small separations and it becomes significantly different at large separations. Different non-identical QD systems are compared quantitatively to highlight the differences in the electronic structures. We conclude that the larger dissimilarity results in the reduced optical gap and increased $e1$ - $e2$. Both of these facts support the use of such systems in the construction of long wavelength optical lasers. Our atomistic tight binding model captures the long range strain effects on the electronic structures which were not present in previous studies using effective mass

approximation [25]. These trends and observations point to the importance of atomistic modeling of realistically extended systems containing around 10 million atoms. The use of quantum dots in the construction of the laser or the optical detector and in the quantum computing applications may likely contain more dots and extend over system of ~ 50 million atoms.

ACKNOWLEDGEMENTS

This work was carried out in part at the Jet Propulsion Laboratory (JPL), California Institute of Technology, under a contract with the National Aeronautics and Space Administration. Muhammad Usman is funded through Fulbright USAID (Grant ID # 15054783). nanohub.org [28] computational resources were used in this work.

REFERENCE

- [1] Y. Arakawa and H. Sakaki, Appl. Phys. Lett. 40, 939 (1982)
- [2] B. Bayer, P. Hawrylak, K. Hinzer, S. Fafard, M. Korkusinski, R. Wasilewski, O. Stern and A. Forchell, Science, 291, 451 (2001)
- [3] G.S. Solomon et al., Phys. Rev Lett. 76, 952 (1996)
- [4] Q. Xie, A. Madhukar, P. Chen and N. P. Kobayashi, Phys. Rev Lett., 75, 2542 (1995)
- [5] O. Stier, M. Grundmann and D. Bimberg, Phys. Rev Lett., 59, 5688, (1999)
- [6] Olga L. Lazarenkova, et al., Appl. Phys. Lett. 85, 4193 (2005)
- [7] J.J. Palacios and P. Hawrylak, Phys. Rev B, 51, 1769 (1995); A. Schliwa, O. Stier, R. Heitz, M. Grundmann and D. Bimberg, Phys. Status Solidi B 224, 405 (2001)
- [8] W. Jaskolski, M. Zielinski, G. W. Bryant and J. Aizpurua, Phys. Rev B, 74, 195339 (2006)
- [9] G. Bester, J. Shumway and A. Zunger, Phys. Rev Lett., 93, 047401 (2004); L. He and A. Zunger, Phys. Rev B, 75, 075330 (2007)
- [10] L. He and A. Zunger, Phys. Rev. B 75, 075330 (2007)
- [11] M. Korkusinski and G. Klimeck, Journal of Physics: Conference Series Vol. 38, pg 75-78 (2006)
- [12] G. Klimeck et al., (INVITED) special issue on NanoElectronic device modeling in IEEE Trans. on Elect. Device (Part II), Vol 54 issue 9 (2007) pg: 2090-2099
- [13] G. Klimeck et al., (INVITED) special issue on NanoElectronic device modeling in IEEE Trans. on Elect. Device (Part I), Vol 54 issue 9 (2007) pg: 2079-2089
- [14] G. Klimeck et al., Superlattices and Microstructures vol. 31/2, pg:171-179 (2002)
- [15] T. Boykin et al., Phys. Rev. B 66, 125207 (2002)
- [16] P. Keating, Phys. Rev. vol 145, no 2 pg: 637-644 (1966)
- [17] R.C. Bowen et al., J. of Appl. Physics 81, 3207 (1997)
- [18] S. Lee et al., Phys. Rev. B 66, 235307 (2002)
- [19] R. Rahman et al., Phys. Rev. Lett. Vol. 99 pg:036403 (2007)
- [20] N. Kharche et al., Appl. Phys. Lett. Vol 90, 092109 (2007)
- [21] M. Usman et al., in proc. 28th ICPS, Vienna, Austria Jul. 24-28 (2006)
- [22] S. Ahmed et al., in proc. of IEEE NEMS, Bangkok Thailand Jan 16-19 (2007)
- [23] W. Sheng et al., Appl. Phys. Lett. 81, 4449 (2002)
- [24] M. Grundmann et al., Phys. Rev. B 52, 11969 (1995)
- [25] M. Rotani et al., Solid State Commun. 119, 309 (2001)
- [26] E. A. Stinaff et al., Science 311, 636 (2006)
- [27] K. Kuldova, V. Krapek, A. Hospodkova, J. Oswald, J. Pangrac, K. Melichar, E. Hulcius, M. Potemski, and J. Humlicek, Phys. Stat. Sol. (c) 3 (2006) 3811.
- [28] <http://www.nanohub.org>